GEOMORPHOMETRY 2020 PERUGIA, ITALY JUNE 22 - 26 2020

Quantifying geomorphic change in a partially restored gully using multitemporal UAV surveys and monitoring discharge and sediment production

Alberto Alfonso-Torreño[§], Álvaro Gómez-Gutiérrez, Susanne Schnabel
Research Institute for Sustaniable Land Development (INTERRA)
University of Extremadura, Cáceres, Spain
[§] albertoalfonso@unex.es

Abstract—**Gully erosion in valley bottoms is a frequent process with negative consequences in the landscape. The development of new techniques and instruments allows the study of gullied channels with high spatial and temporal resolution. Here we present a detailed study of a valley bottom gully that was restored in 2017 with check dams. The channel is located in an experimental catchment, which is equipped with sensors to continuously monitor rainfall, discharge and suspended sediment concentration. The objectives of this work are (1) to analyze the effectiveness of operations carried out in the channel and (2) to elucidate the role of the former operations on the hydrological and sedimentological spatial and temporal dynamic. The methodology included the following steps: 1) field survey with a fixed-wing UAV to capture high-resolution aerial photographs and a GNSS to provide Ground Control Points (GCPs), 2) Structure-from-Motion photogrammetry to produce multi-temporal point clouds, DEMs and orthophotographs, 3) estimating topographic changes and 4) analyzing the relationship between rainfall and discharge events, sediment load and topographic changes. A spatially variable threshold was produced using a Fuzzy Inference System and considering different sources of errors. For the period 2017-2019 (i.e. after restoration activities), the gully showed a positive balance indicating accumulation of sediments (40.2 m^3) and hence a good performance of the restoration measures. The sediment load was reduced after dams installation, while runoff was not modified.**

I. Introduction

Gully erosion is one of the erosive processes that mostly contributes to shape the Earth surface. In fact, gully erosion represents one of the most significant types of soil degradation in the dehesa landscape, an agrosilvpoastoral land use system widespread in the SW Iberian Peninsula. Gullies are located in valley bottoms and studies have quantified the magnitude of these processes in a dehesa environment, determining for the period 2001-2007 an average gully erosion rate of 4.17 $m^3\ y^{-1}$ [1]. Among the different restoration strategies, check dams are often used in Mediterranean areas [2-5]. Nevertheless, there are still few studies monitoring the effects of check dams on sediment dynamics [4].

In the last decade, recent advances in airborne-based surveying technologies, transformed the topographic data acquisition, replacing the method based on interpolating cross sections to estimate the volumetric change in channels [1, 6, 7]. The recent development of UAV platforms facilitates the acquisition of high resolution aerial photos from which Structure-from-Motion [8] photogrammetry can be applied to obtain point clouds, DEMs and orthophotos, being very useful to analyze geomorphic changes in gullies [9-10]. Geomorphic changes can be monitored through repeated and low-cost topographic surveys [11-12]. A DEM of differences (DoD) [13] is relevant to geomorphic studies because it provides a spatially distributed model of topographic change through time [14-15]. Uncertainties in topographic representation of a surface in a DEM have implications for DEM applications, these uncertainties or error can be considered as a spatially variable threshold. Several studies characterized error as being uniform across the entire DEM surface [14, 16]. Fuzzy inference systems (FIS) [17] allow estimating topographic changes from multiple factors that contribute to DEM uncertainty [13, 18]. The present work aims to analyze the effectiveness of operations carried out in the channel and to clarify the role of the former measures in the hydrological and sedimentological spatial and temporal dynamic of the gullied channel. Five high-resolution DEMs and orthophotographs were obtained from 2016 to 2019. In February 2017 (i.e. after the first survey) the gully was restored with check dams. Additionally, rainfall, discharge and suspended sediment were continuously monitored at the outlet of the catchment.

II. Study Area

The study was conducted in the Parapuños experimental catchment (99.5 ha) in the SW of the Iberian Peninsula (Fig. 1). The area is representative of the dehesa land use system. The

Alberto Alfonso-Torreno, Alvaro Gomez-Gutierrez and Susanne Schnabel (2020)
Quantifying geomorphic change in a partially restored gully using multitemporal UAV surveys and monitoring discharge and sediment production:
in Massimiliano Alvioli, Ivan Marchesini, Laura Melelli & Peter Guth, eds., Proceedings of the Geomorphometry 2020 Conference, doi:10.30437/GEOMORPHOMETRY2020_54.

channel is a second order stream, which in the lower part of the catchment is incised into alluvial sediments. The main gully has a length about 850 m. Climate is Mediterranean with an average annual temperature of 16ºC and an average annual rainfall of 600 mm with high seasonality. The average altitude of the catchment is 396 m a.s.l. and the mean slope is 8%. The vegetation cover is composed of a disperse layer of Holm oak (*Quercus ilex va. rotundifolia*) and herbaceous plants in the understory. Livestock rearing is the main land use in the study area, with sheep and cows. Three different subsections were considered in the channel: (1) upper reach with restoration measures built in February 2017; (2) lower reach and (3) tributary reach.

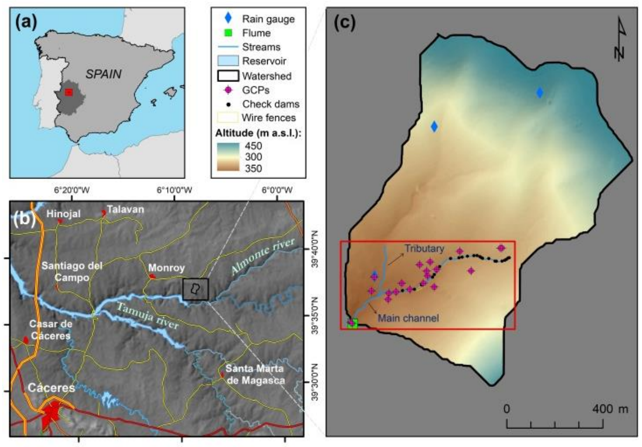

Figure 1. (a) Location of the study area in the Iberian Peninsula, (b) regional setting of the study area and (c) the gullied channel area represented by a red rectangle, including check dams and the GCPs represented by pink points.

III. MATERIAL AND METHODS

A. Monitoring rainfall, discharge and suspended sediment

The location of the measurement tools in the study area is presented in Figure 1c. The catchment is equipped with three tipping bucket rain gauges that recorded with a resolution of 0.2 mm at 5 minute intervals. Discharge was determined using a water depth probe installed in a weir at the outlet of the watershed, allowing measurement of a wide range of discharges (1-4000 l s^{-1}). Data analysis was conducted at different temporal scales: rainfall event, month and year. An event database was elaborated including rainfall events that generated runoff between September 2013 and August 2019. For event separation, a minimum period between two events of 1 hour without precipitation was used. The separation of base flow from direct runoff was through the technique of the normal depletion curve [19]. Flood discharges were identified as a flow increase of at least 1.5 times base flow prior to the rainfall event. At the event scale the following variables were used: antecedent rainfall, rainfall intensity, discharge (flood and base flow) and runoff coefficient (RC).

B. Field surveys and SfM workflow

The SfM-MVS workflow was fed with aerial photographs acquired by a fixed-wing UAV (Ebee by Sensefly) carrying on board a Sony WX220 sensor (18 Mpx). A total of 5 flights were conducted (24/03/2016, 16/02/2017, 25/10/2017, 03/05/2018 and 25/01/2019). Twenty GCPs were registered with a GNSS and used to scale and georeference the models (Fig. 1c). Pix4D software was used to process the UAV-derived photographs to produce point clouds, high-resolution DEMs and orthophotos.

C. DEMs of Difference and error analysis

Geomorphic change analysis was conducted through the DEM of difference approach [13], using the Geomorphic Change Detection (GCD) v7.1 add-in within ArcGIS Desktop v10.6. The DoD approach is based on the georeferencing error and the spatially variable error. The fuzzy inference system (FIS) method [13] was used to evaluate spatially variable errors. A two-input rule FIS system based on DEM slope and canopy height model (CHM) are used as indicators of vertical uncertainty. A third variable related to grassland was included applying a minimum level of detection (minLoD) based on the height of the grass in the different periods analyzed. The behavior of each variable on the final spatially variable error surface depends on the pre-designed membership functions. The process of defining membership functions for a variable can be thought of in two parts. First, the number of classes was identified (low, medium and high) to characterize the variable being described. Finally define the membership function that will describe the range of values covered by each class for the input or output. The total consequence membership function resulted in a raster output with values about elevation uncertainties. The FIS output used default MFs for the uncertainty (δz) and output was categorized into four classes (Low, Average, High, Extreme). Finally, a map of spatially vertical uncertainty (δz) of each DEM was obtained. Then, the elevation errors of each DEM were quantified in the DoD as described by [16, 20], with the following equation:

$$minLoD = t\,(\delta z_{DEMnew}{}^{2} + \delta z_{DEMold}{}^{2})^{0.5} \qquad (1)$$

where the minLoD is the critical threshold in the DoDs of significant topographic change for a 95% confidence interval, and σZ_{DEMnew} and σZ_{DEMold} are estimated uncertainties of the two compared DEMs. Topographic change was only considered in values greater than values of the error surface. Significant topographic changes were detected spatially and erosion and deposition volumes were calculated by multiplying the value by the pixel size of the resulting raster.

IV. RESULTS

A. Photogrammetric results

A total of 5 point clouds with a volumetric point density of 1504 pts m^3 on average were obtained and DEMs and orthophotographs with a GSD of 0.02 m resulted from the SfM processing. The total processing time (of the five models) for point clouds, Digital Terrain Model (DTM) and orthopotograph generations was almost 20 hours.

B. Geomorphic change in the gully

A total accumulation of 98.3 m^3 in the channel was estimated for the period 2016-2019, representing an annual deposition rate of 34.6 m^3 y^{-1}. Geomorphic change showed a high temporal variability, from -40.4 m^3 of net erosion experienced in P2 to 88.8 m^3 of net deposition during P3 (Table 1). All recorded-monitored variables experienced high temporal variability. The rainfall ranged from 476 mm (P3) to 182 mm (P2). The flood discharge ranged from 37277 m^3 in P3 (6 events with a Q > 100 l s^{-1}) to 3622 m^3 in P4 (1 event with a Q > 100 l s^{-1}). The largest amount of sediments was registered in P2 with 99.2 tons. The statistical analysis showed significant relationships between several variables (Table 2). Erosion-deposition values were highly correlated with rainfall, flood discharge, number of times Q > 100 l s^{-1} and maximum rainfall intensity in 60 minutes.

Table 1. Summary of the data registered during the study period: erosion or deposition, net volume difference (NVD), rainfall (P), flood discharge (Q), maximum peak discharge, the number of times discharge exceeding 100 l s^{-1}.

Period	**P1**	**P2**	**P3**	**P4**
Duration	24/03/2016 - 16/02/2017	16/02/2017 - 25/10/2017	25/10/2017 - 03/05/2018	03/05/2018 - 25/01/2019
Erosion (m^3)	-10.0	-46.7	-1.3	-14.9
Deposition (m^3)	65.7	6.3	90.2	6.6
NVD (m^3)	55.7	-40.4	88.8	-8.3
Rainfall (mm)	446.6	181.7	476.2	328.1
Events (N)	28	3	25	19
P mean (mm)*	11.0	26.1	11.5	10.1
Q (m^3)*	20165.1	18218.1	37277.4	3622.3
Q-max (l s^{-1})*	541.6	1237.2	1052.3	336.7
Q > 100 l s^{-1} (N)*	2	1	6	1
I60 (mm)*	4.7	8.8	4.1	6.4
RC (%)*	3.8	12.5	6.0	2.1
Sed. load (t)*	37.8	99.2	20.6	1.9

(*) Event scale

Table 2. Correlation matrix for NVD, rainfall, flood discharge (Q), maximum peak flood (Q-max), RC, sediment load and maximum 60-minutew rainfall (I60). Statistically significant values ($p < 0.05$) are highlighted

	NVD *(m^3)*	Rain *(mm)*	Q *(m^3)*	Q-max *l s^{-1}*	Q > 100 *(N)*	I-60 *(mm)*	RC *(%)*
Rainfall	**0.87**						
Flood discharge (m^3)	**0.88**	**0.59**					
Q-max (l s^{-1})	0.31	**0.55**	**0.90**				
Q > 100 l s^{-1} (N)	**0.92**	0.34	0.52	**0.68**			
I-60 (mm)	-0.11	**0.57**	0.22	0.37	0.35		
RC (%)	-0.16	0.38	**0.85**	**0.87**	**0.57**	0.14	
Sed load (kg)	-0.51	0.48	**0.84**	0.66	0.39	0.11	**0.55**

Different processes were observed in the gully, dominating the aggradation processes as determined by the topographic change analysis. Channel aggradation processes were observed, filling the channel bed and forming sediment bars at different locations along the gully, but also in the installed check dams. The source areas of these sediments are the hillslopes where sheet erosion takes place. Several erosion processes were also observed: a) channel bed erosion, due to the direct action of water flow and transported materials, b) lateral bank erosion and bank collapse produced by lateral incision followed by the collapse of the upper part of the banks, c) deepening and widening in a few headcuts where the tributary and the lower reach join and d) erosion downstream of the check dams. Only two lateral headcuts were advancing during P4.

C. Effectiveness of restoration measures

The total volume of sediments retained in the check dams are 11.7 m^3 from which 85% are accumulated in permanent check dams. The total volume of sediments accumulated in the check dams represents 12.4% of the upper reach deposition. Of the three periods analyzed with the restoration measures, the check dams in P4 did not retain sediments, it is a period characterized by net erosion. Nearly half of the total sediment volume (49%) retained in the check dams occurred in P2. During this period an event with 49.3 mm and a maximum flow of 1237.2 l s^{-1} occurred, producing a flood discharge of 18,136.7 m^3 which was the highest maximum flood registered since 2009-10.

Regarding sediment load at the outlet of the catchment, sediments transported in the channel came from two sources, the hillslopes (due to sheet erosion) and the valley bottoms (due to gully erosion). The average annual sediment load was 73.8 tons, equivalent to 0.72 t ha^{-1} y^{-1}. The interannual variation is very high, ranging from 0.07 to 1.86 t ha^{-1} y^{-1}. The first year after check dam's construction 561 mm of rainfall was recorded, generating 56,743 m^3 of discharge with a RC of 10.3%. This was the year with the third highest value of the RC, being the seventh highest in sediment production. Figure 2 presents the relationship between suspended sediment load and flood discharge which are significantly correlated. This analysis shows how sediment production was clearly reduced by the presence of check dams

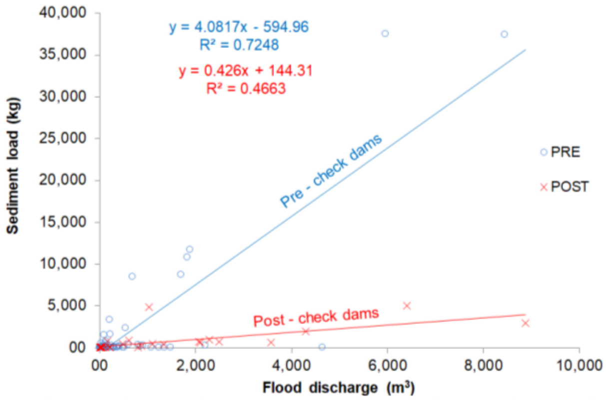

Figure 2. Relationship between flood discharge and sediment load depending on events pre or post check-dams.

V. CONCLUSIONS

Multi-temporal topographic (UAV+SfM photogrammetry) surveys have allowed us to analyze the effectiveness of restoration measures conducted in the channel and to study the hydrological and sedimentological dynamic after check dams' construction. Topographic changes were determined through the DEM of difference approach. The fuzzy inference system method was used to evaluate spatially variable errors. A total accumulation of 98.3 m^3 in the channel was estimated for the period 2016-2019. For the period after check dams construction, the gully showed a positive balance of 40.2 m^3 demonstrating the effectiveness of the restoration measures. Sediment load was reduced after check dam installation, though not affecting runoff generation. These results are valuable to quantify the magnitude of the erosive processes in dehesa landscapes and to understand the role of restoration measures in gullies.

ACKNOWLEDGMENTS

Alfonso-Torreño is a beneficiary of a PhD scholarship (PD16004) of the Regional Government of Extremadura and research was financed by the Spanish Ministry of Economy and Competitiveness (CGL2014-54822-R).

REFERENCES

[1] Gómez-Gutiérrez, Á., Schnabel, S., De Sanjosé, J.J., Lavado Contador, J.F., 2012. "Exploring the relationships between gully erosion and hydrology in rangelands of SW Spain". Zeitschrift für Geomorphologie, Supplementary Issues 56, 27–44.

[2] Castillo, V.M., Mosch, W.M., Conesa García, C., Barberá, G.G., Navarro Cano, J.A., López-Bermúdez, F., 2007. "Effectiveness and geomorphological impacts of check dams for soil erosion control in a semiarid Mediterranean catchment: El Cárcavo (Murcia, Spain)". Catena 70 (3), 416-427.

[3] Bombino, G., Gurnell, A.M., Tamburino, V., Zema, D.A., Zimbone, S.M., 2009. "Adjustements in cannel form, sediment calibre and vegetation around check-dams in the headwater reaches of mountain torrents, Calabria, Italy". Earth Surface Processes Landforms 34 (7), 1011-1021.

[4] Cucchiaro, S., Cavalli, M., Vericat, D., Crema, S., Llena, M., Beinat, A., Marchi, L., Cazorzi, F., 2019. "Geomorphic effectiveness of check dams in a debris-flow catchment using multi-temporal topographic surveys". Catena 174, 78-83.

[5] Alfonso-Torreño, A., Gómez-Gutiérrez, Á., Schnabel, S., Lavado Contador, J.F., Sanjosé Blasco, J.J., Sánchez Fernández, M., 2019. "sUAS, SfM-MVS photogrammetry and a topographic algorithm method to quantify volume of sediments retained in check-dams". Science of the Total Environment 678, 369-382.

[6] Griffiths, G.A., 1979. "Recent sedimentation history of the Waimakariri River, New Zealand". Journal of Hydrology (New Zealand), 18: 6-28.

[7] Ferguson, R., Ashworth P.J., 1992. "Spatial patterns of bedload transport and channel change in braided and near-braided rivers". In: Dynamics of Gravel-bed Rivers, Billi P, Hey RD, Thorne CR, Tacconi P (Eds). John Wiley & Sons Ltd; 477-492.

[8] Ullman, S., 1979. "The interpretation of structure from motion". Proceedings of the Royal Society B, 203, 405-426.

[9] Castillo, C., Pérez, R., James, M.R., Quinton, J.N., Taguas, E.V., Gómez, J.A., 2012. "Comparing the accuracy of several field methods for measuring gully erosion". Soil Science Society of America Journal 76, 1319.

[10] Gómez-Gutiérrez, Á., Schnabel, S., Berenguer-Sempere, F., Lavado-Contador, F., Rubio-Delgado, J., 2014. "Using 3D photo-reconstruction methods to estimate gully headcut erosion". Catena 120, 91–101.

[11] Xiang, J., Chen, J., Sofía, G., Tian, Y., Tarolli, P., 2018. "Open-pit mine geomorphic changes analysis using multi-temporal UAV survey". Environmental Earth Sciences 77, 220.

[12] Kaiser, A., Erhardt, A., Eltner, A., 2018. "Addressing uncertainties in interpreting soil surface changes by multitemporal high-resolution topography data across scales". Land Degradation & Development 29 (8), 2264-2277.

[13] Wheaton, J.M., Brasington, J., Darby, S.E., Sear D.A., 2010. "Accounting for uncertainty in DEMs from repeat topographic surveys: improved sediment budgets". Earth Surface Processes and Landforms 35, 136-156.

[14] Brasington, J., Langham, J., Rumsby, B., 2003. "Methodological sensitivity of morphometric estimates of coarse fluvial sediment transport". Geomorphology 53 (3–4), 299–316.

[15] Rumsby, B.T., Brasington, J., Langham, J.A., McLelland, S.J., Middeton, R., Rollinson, G., 2008. "Monitoring and modelling particle and reach-scale morphological change ingravel-bed rivers: applications and challenges". Geomorphology 93, 40–54.

[16] Brasington, J., Rumsby, B., McVey, R., 2000. "Monitoring and modelling morphological change in a braided gravel-bed river using high resolution GPS-based survey". Earth Surf. Processes Landforms 25 (9), 973–990.

[17] Milan, D.J., Heritage, G.L., Large, A.R.G, Fuller, I.C., 2011. "Filtering spatial error from DEMs: Implications for morphological change estimation". Geomorphology 125, 160-171.

[18] Prosdocimi, M., Calligaro, S., Sofia, G., Dalla Fontana, G., Tarolli, P., 2015. "Bank erosion in agricultural drainage networks: New challenges from structure-from-motion photogrammetry for post-event analysis". Earth Surface Processes Landforms 40 (14), 1891–1906.

[19] Horton, R.E., 1933. "The role of infiltration in the hydrologic cycle". Transactions, American Geophysical Union 14, 446–460.

[20] Lane, S. N., Westaway, R. M., & Murray Hicks, D., 2003. "Estimation of erosion and deposition volumes in a large, gravel-bed, braided river using synoptic remote sensing". Earth Surface Processes and Landforms 28, 249–271.